

Microstructure and Phase Transition of ZnO Varistor Ceramics

Kyung-Nam Kim and Sang-Mok Han

Dept. of Materials Engineering, Kangwon National Univ.

(Received November 23, 1990)

ZnO바리스터 세라믹스의 미세구조와 상전이

김경남 · 한삼목

강원대학교 재료공학과

(1990년 11월 23일 접수)

ABSTRACT

Microstructure and phase changes during the sintering of ZnO varistors were studied in ZnO-Bi₂O₃-CoO-Sb₂O₃ and ZnO-Bi₂O₃-CoO-Sb₂O₃-Cr₂O₃ systems using scanning electron microscopy (SEM) with an energy dispersive X-ray analysis (EDAX), X-ray diffraction (XRD) and differential thermal analysis (DTA).

The spinel phase and the Bi₂O₃ phase were formed by the decomposition of the pyrochlore phase during heating. The spinel particles (2-4μm), which were formed both along the grain boundaries and within the ZnO grain, were always found near the pyrochlore phase. Intergranular phases (Bi₂O₃ and pyrochlore) were precipitated from the liquid phase during cooling. The Bi₂O₃ phases were located at the triple (or multiple) point of the ZnO grains. Cr₂O₃ played a role in decreasing the formation temperature of the spinel phase and Bi₂O₃ phase during sintering, and inhibited the grain growth.

요 약

ZnO 바리스터의 소결과정에서 상변화와 미세구조는 여러분 석기기(SEM/EDAX, XRD와 DTA)를 이용하여, ZnO-Bi₂O₃-CoO-Sb₂O₃와 ZnO-Bi₂O₃-CoO-Sb₂O₃-Cr₂O₃계에서 조사하였다.

Spinel상과 Bi₂O₃상은 소결 과정에서 pyrochlore상의 분해에 의해 형성되었다. Spinel입자(2-4μm)들은 ZnO입자들 사이의 ZnO입자내에 놓여 있었으며, 항상 pyrochlore상과 인접하게 위치하고 있었다. Intergranular(Bi₂O₃, pyrochlore)상들은 고온에서 냉각동안 액상에 의해 나타나며, Bi₂O₃상은 ZnO입자들의 triple(또는 multiple) point에 위치한다. Cr₂O₃는 소결 과정에서 spinel과 Bi₂O₃상의 생성온도를 낮추며, 입자성장을 억제하였다

1. INTRODUCTION

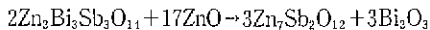
Zinc oxide ceramics with a small addition of Bi₂O₃ and several other oxides show a highly non-ohmic

behavior in the current-voltage characteristics¹. They have been widely used as surge arrestors and stabilizers in electric power system and electronic circuits^{2,3}.

The microstructure of ZnO varistor which was composed of ZnO grains, spinel and Bi-rich intergranular phases (Fig.1) is known to have an important effect on the non-ohmic characteristics and other electrical properties.

In the early studies^{1,2,3)} of ZnO varistors, it was believed that continuous intergranular layers of high-resistivity (Bi_2O_3 ⁶⁾, $\rho \approx 10^{13} \Omega \cdot \text{cm}$), which isolate the ZnO grains completely, were responsible for the non-ohmic behavior. However, later investigations⁷⁾ using direct observation in the transmission electron microscope have shown that the intergranular phase was not continuous but isolated at triple points of the ZnO grains

The spinel phase ($\text{Zn}_7\text{Sb}_2\text{O}_{12}$) in the $\text{ZnO}-\text{Bi}_2\text{O}_3-\text{Sb}_2\text{O}_3$ system was formed by the decomposition of the pyrochlore ($\text{Bi}_2(\text{Zn}_{1/3}\text{Sb}_{2/3})\text{O}_6$ ⁸⁾, $\text{Bi}_{3/2}\text{ZnSb}_{3/2}\text{O}_7$ ⁹⁾) phase according to the following reaction.



Wong⁹⁾ first reported that the ratio of the spinel to pyrochlore increases with the sintering temperature. Inada⁹⁾ has proposed that the phases present in ZnO varistors varied with cooling rate and amount of the transition metal oxide. Also, the spinel and pyrochlore phase have been identified in the ZnO varistors by the several investigators⁸⁻¹⁰⁾ during the last decade. Very little published work has been done,

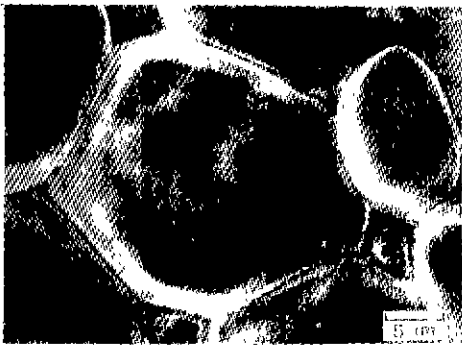


Fig.1. Scanning electron micrograph of $\text{ZnO}-\text{Bi}_2\text{O}_3-\text{CoO}-\text{Sb}_2\text{O}_3$ system sintered at 1250°C .

however, on the studies of the reaction between the spinel and pyrochlore phase during sintering of the ZnO varistors. The spinel and pyrochlore phase may affect the electrical properties through their effects on the microstructure development during sintering. So, it is desirable to have a better understanding of the formation reactions of spinel and pyrochlore phase.

In this study, the microstructural features of the phases (spinel, pyrochlore) and phase transformation during heating in the $\text{ZnO}-\text{Bi}_2\text{O}_3-\text{CoO}-\text{Sb}_2\text{O}_3$ and $\text{ZnO}-\text{Bi}_2\text{O}_3-\text{CoO}-\text{Sb}_2\text{O}_3-\text{Cr}_2\text{O}_3$ systems are studied to understand clearly the reaction between the spinel and pyrochlore phase

2. EXPERIMENTAL PROCEDURE

Sample preparation—The raw materials used in this study were reagent-grade powders of ZnO^* , $\text{Cr}_2\text{O}_3^{**}$, $\text{Bi}_2\text{O}_3^\dagger$, CoO^\ddagger and $\text{Sb}_2\text{O}_3^{+\dagger}$. The samples were prepared by conventional ceramic process¹¹⁾. The composition of sample (a) was 97.5 ZnO containing 1.0 Bi_2O_3 , 0.5 CoO , and 1.0 Sb_2O_3 in mole ratio and the composition of sample (b) was 96.5 ZnO, 1.0 Bi_2O_3 , 0.5 CoO , 1.0 Sb_2O_3 and 1.0 Cr_2O_3 .

The powders were ball milled with distilled water for 10 hr and were dried at 80°C for 24 hr, and powders were granulated using 80 mesh sieve to improve the flow characteristic. These powders were formed into the disc shape with the pressure of 1000 kg/cm^2 and sintered by the heating schedule as shown in Fig.2. Finally the sintered specimens were quenched at the desired temperatures.

XRD—The crystal phases present in each specimen were examined by the X-ray diffraction (XRD, Philips Co. PW1710) as the powder method using $\text{CuK}\alpha$ radiation.

* G R grade, ** 1st grade, Junsei Chem. Co., Ltd. (Japan)

† 99.9%, Janssen Chem. Co., Ltd. (Belgium)

‡ G R grade, Kanto Chem. Co., Ltd (Japan)

+† 1st grade, Kokusan Chem. Co., Ltd. (Japan)

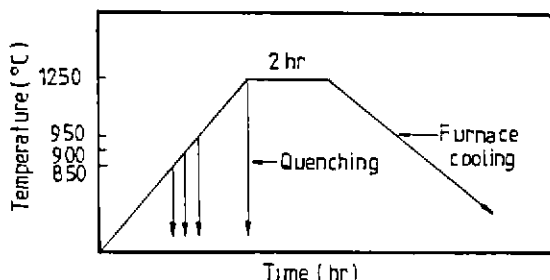


Fig. 2. Thermal schedule of sintering.

SEM/EDAX—The examination of the microstructural features of the each phases was carried out using the scanning electron microscopy (SEM, Hitachi Co. X-650) with the energy dispersive X-ray analysis (EDAX).

DTA—An appropriate fine powder (320 mesh) was analyzed by the differential thermal analysis (DTA, Rigaku Co. PTC-10A). Powders were heated to 1100°C with the heating rate of 10°C/min in an air environment. The reference material was α -Al₂O₃.

Grain size—The average grain sizes were measured by the intercept method¹³⁾, which was calculated by counting the number of grain boundaries intercepted by the line of known length.

3. RESULTS AND DISCUSSION

3.1. PHASE CHANGE

XRD analysis—Fig. 3 shows the X-ray diffraction patterns of the samples which were quenched at 850°C. Whereas phases present in the sample (a) were ZnO grains, pyrochlore and poor spinel phases, sample (b) showed Bi₂O₃ phase also. The pyrochlore

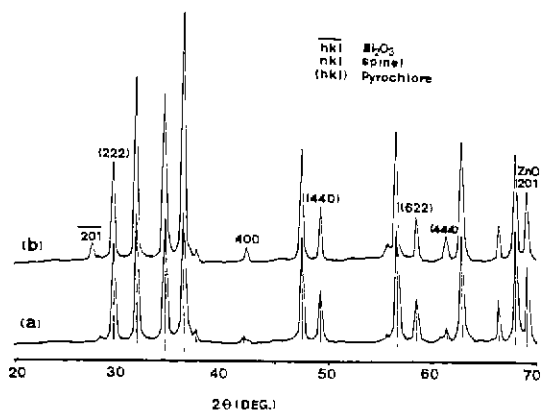


Fig. 3. X-ray diffraction patterns of samples quenched at 850°C.

- (a) ZnO-Bi₂O₃-CoO-Sb₂O₃,
- (b) ZnO-Bi₂O₃-CoO-Sb₂O₃-Cr₂O₃.

phase was formed at temperatures below 850°C in the both samples. The Bi₂O₃ and spinel phases were appeared at 850°C in sample (b), while the poor Bi₂O₃ phases detected at 900°C in sample (a).

Fig. 4 shows ratios of the X-ray peak height Bi₂O₃ (201), spinel (400), and pyrochlore (222, 440) phase to that of ZnO (201), respectively. At 850–950°C, in the sample (a), the peak heights of the pyrochlore phase have increased. On the other hand, in the sample (b), peak heights of the pyrochlore phase have decreased, but peak heights of the spinel and Bi₂O₃ phase have increased.

In the samples sintered at 1250°C, a ZnO grains, Bi₂O₃ and spinel phase were present. It is noticeable that the samples in which were cooled slowly, pyrochlore phase was detected (Table 1). The X-ray intensities of spinel, pyrochlore and Bi₂O₃ phases were dependent on the firing temperature as well as on the additive oxides.

DTA analysis—Fig. 5 shows the differential thermal analysis (DTA) patterns of the two system powders.

The endothermic peaks were observed around 910°C in sample (a) and around 820°C in sample (b). These temperatures almost coincide with the spinel phase formation temperatures as shown in Fig. 4 (see X-ray

Table 1. Phase Formation in the Samples Heated at Various Temperatures.

temp samp.	850°C	900~950°C	1250°C (q)	1250°C (s)
(a)	Z+P+S	Z+S+P+B	Z+S-B	Z+P+S+B
(b)	Z+P+S+B			

Z ZnO, P pyrochlore, S spinel, B Bi₂O₃.

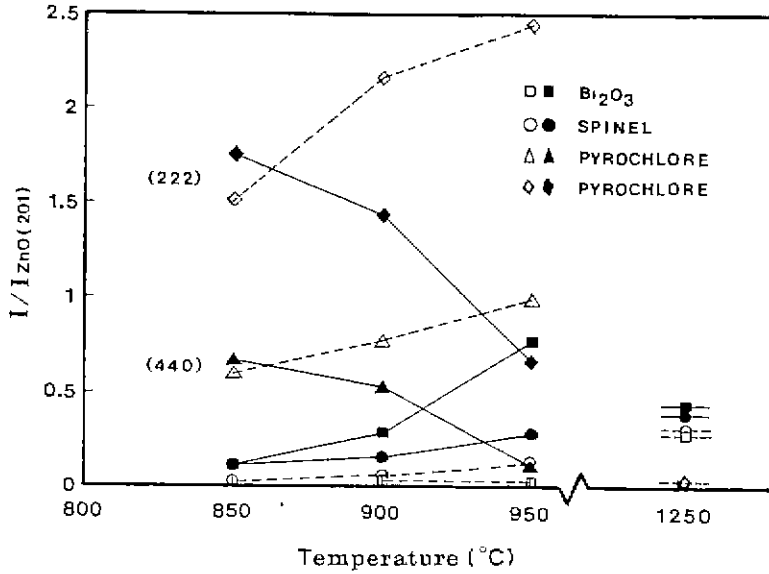


Fig.4. X-ray peak heights for Bi₂O₃(201), spinel(400) and pyrochlore(222, 440) phase as compared to ZnO(201) (— ZnO-Bi₂O₃-CoO-Sb₂O₃-Cr₂O₃ system, ---- ZnO-Bi₂O₃-CoO-Sb₂O₃ system).

results). The sample (a) shows sharp endothermic peak, whereas the sample (b) shows broad endothermic peak. In addition, the endothermic reaction in sample (b) starts from lower temperature than that of sample (a).

The results presented in Fig.3, 4(XRD) and Fig. 5(DTA) can be explained as follows. The pyrochlore phase was formed during heating. The spinel and Bi₂O₃ phase were formed by the decomposition of the pyrochlore phase. The Bi₂O₃ phase were formed at 850°C in sample (b) and at 900°C in sample (a), respectively. The Cr₂O₃ seemed to lower the formation temperature of the spinel and Bi₂O₃ phase.

These results are similar to the previous researchers^{9,10} which showed the DTA results of the varistor materials Inada⁹ also showed that a pyrochlore was formed at 900°C during heating and the additions of the transition metal oxides decreased the formation temperature of spinel and Bi₂O₃ phase.

Imai¹⁰ reported that because the pyrochlore phase has a defective structure, the additive oxides(SiO₂ and

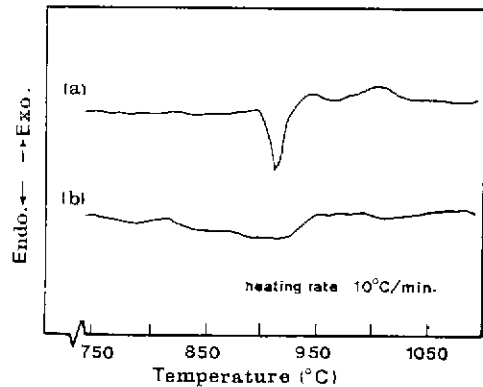


Fig.5. Differential thermal analysis curves for starting powders.

(a) ZnO-Bi₂O₃-CoO-Sb₂O₃,

(b) ZnO-Bi₂O₃-CoO-Sb₂O₃-Cr₂O₃.

Cr₂O₃) could be dissolved into the pyrochlore, their dissolution would make the structure unstable.

3.2. MICROSTRUCTURE

SEM/EDAX analysis—Fig.1 shows the microstructure of the sample (a) which was sintered at 1250°C

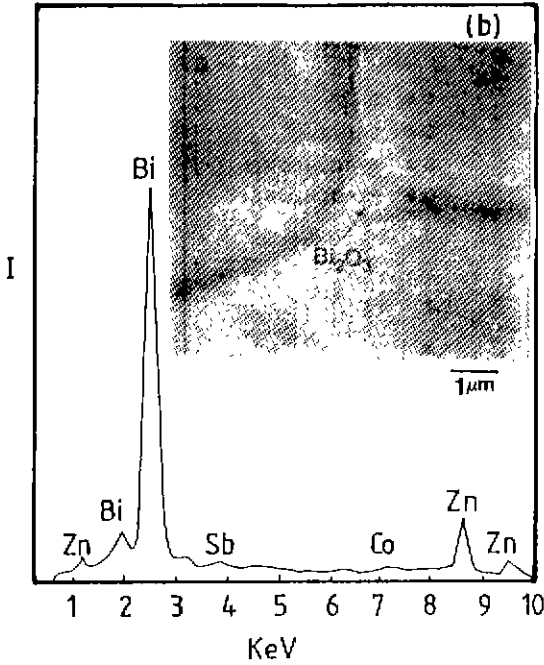


Fig. 6. (a) Morphology of the Bi_2O_3 phase in Fig. 1. (b) EDAX spectrum of Bi_2O_3 phase taken from the triple junction.

ZnO, grains Bi_2O_3 , pyrochlore (Bi-rich phase) and spinel grains. The spinel grains were surrounded by the pyrochlore phase. Some of the spinel particles were also present within the ZnO grains. Intergranular phases (Bi_2O_3 , pyrochlore) were precipitated from the liquid phase during cooling. The pyrochlore phase was found both at the triple (or multiple) points of ZnO grains and at the grain boundaries, and Bi_2O_3 phases were surrounded by ZnO grains.

Fig. 6 shows the EDAX pattern of the Bi_2O_3 phase (Fig. 1). The Bi_2O_3 phase located at the triple point of the ZnO grains shows that it contains zinc, cobalt and antimony.

Fig. 7(a) shows spinel and pyrochlore phases. In case of the samples which were sintered at 1250°C , above morphology was detected and the pyrochlore phase was always found near the spinel particle. Fig. 7(b) and (c) are the EDAX patterns of the spinel and pyrochlore phase. Whereas the spinel ($\text{Zn}_7\text{Sb}_2\text{O}_{12}$) particles contained only cobalt in sample (a), cobalt and chromium were detected in sample (b)

Fig. 8(a) and (b) show a spinel grain located along grain boundary and a spinel grain within ZnO grain.

and slow cooled. The microstructure consisted of

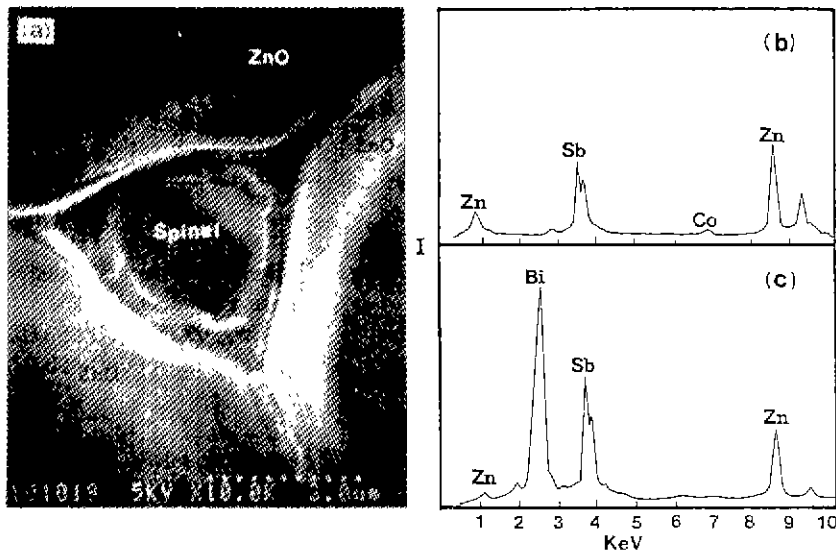


Fig. 7. (a) Scanning electron micrograph of $\text{ZnO}-\text{Bi}_2\text{O}_3-\text{CoO}-\text{Sb}_2\text{O}_3$ system sintered at 1250°C , (b), (c) EDAX spectrum taken from the spinel and pyrochlore phase.

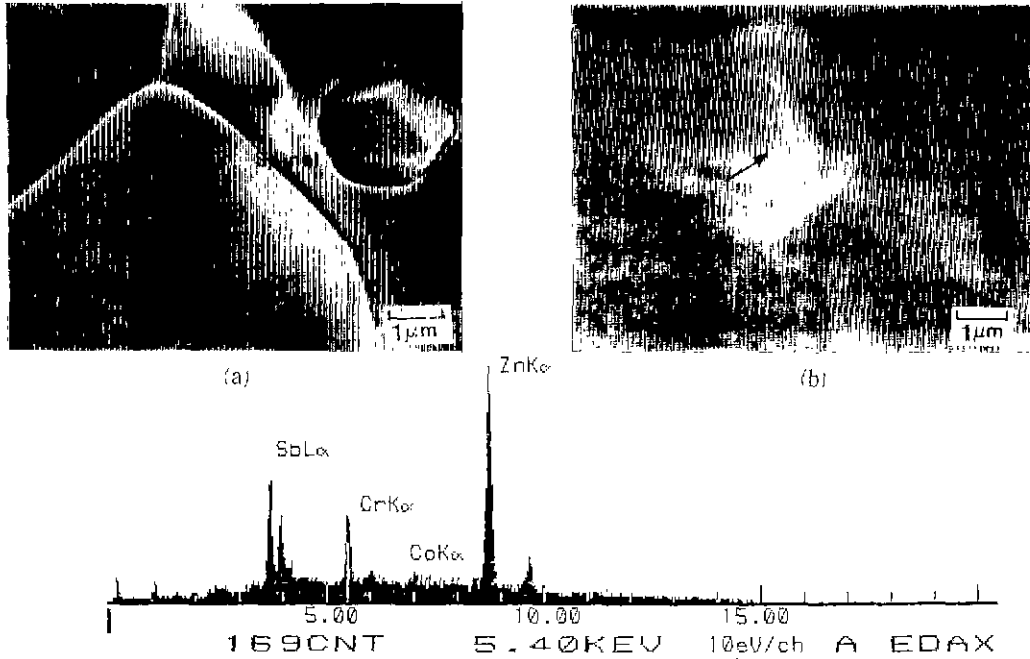


Fig.8. (a), (b) Morphology of the spinel phase taken from the ZnO-Bi₂O₃-CoO-Sb₂O₃-Cr₂O₃ system sintered at 1250°C. (c) EDAX spectrum taken from the spinel phase.

As shown in Fig.8(a), some spinel grains with the pyrochlore phase were present within the ZnO grain. Because spinel particles are too small to be effective as pinning points, spinel particles can be isolated by the migration of the ZnO grain boundaries. Their migration resulted in inclusion such as Bi-rich liquid phase within the ZnO grains. Also, The spinel grains occasionally were in contact directly with ZnO grains.

Fig 8(c) shows an EDAX pattern of the spinel particle. Only dissolved Cr was found in the spinel particle.

Grain growth of ZnO-Fig.9 shows the average ZnO grain sizes of the sintered samples at the various temperatures.

From the above results, the ZnO grain size increased with the sintering temperature. The grain sizes of ZnO in sample (b) were smaller than those of the sample (a).

In the previous observations^{11,12}, ZnO varistor material which contained only Bi₂O₃ as an additive

showed that more addition of Bi₂O₃(0.5~5mol%) results in decrease of the grain sizes. From our present research, it shows that grain growth was

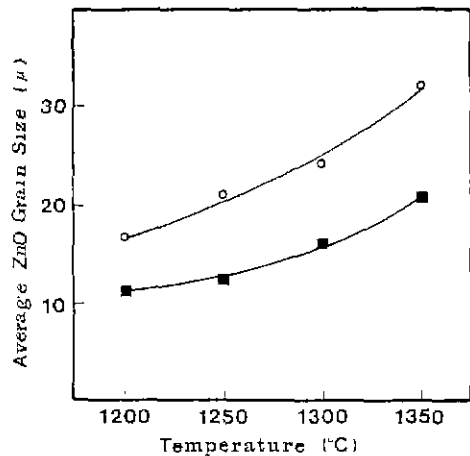


Fig.9. Average ZnO grain size of samples sintered at various temperatures.

- ZnO-Bi₂O₃-CoO-Sb₂O₃,
- ZnO-Bi₂O₃-CoO-Sb₂O₃-Cr₂O₃.

influenced by the spinel and liquid phase Bi_2O_3 which were formed by the decomposition of pyrochlore at the early stage of sintering. The growth of the ZnO grains was controlled by the spinel particles during sintering, because ZnO grain boundaries were pinned by the spinel particles. Thus, the ZnO grain growth occurred coincidentally with the spinel formation. From the results presented in XRD and DTA, because the Cr_2O_3 seemed to lower the formation temperature of the spinel phase, the ZnO grain growth in sample (a) was happened easier than that of in sample (b).

4. CONCLUSION

From the discussion on the microstructure as well as on the phase change in the systems $\text{ZnO}-\text{Bi}_2\text{O}_3-\text{CoO}-\text{Sb}_2\text{O}_3$ and $\text{ZnO}-\text{Bi}_2\text{O}_3-\text{CoO}-\text{Sb}_2\text{O}_3-\text{Cr}_2\text{O}_3$, the following conclusions can be obtained :

1) During the heating, the spinel ($\text{Zn}_7\text{Sb}_2\text{O}_{12}$) and Bi_2O_3 phase appeared at around 850°C . The spinel phase which was formed both in the junctions of the ZnO grains and within the ZnO grain, was found to be always adjacent to a pyrochlore.

2) The intergranular phases (Bi_2O_3 and pyrochlore) were precipitated from the liquid phase during cooling. The Bi_2O_3 phase was located at the triple(or multiple) points of the ZnO grains.

3) The formations of spinel and Bi_2O_3 phase resulted in the decrease of the volume fraction of pyrochlore phase. Cr_2O_3 played a role in decreasing the formation temperature of the spinel phase and Bi_2O_3 phase, and prevented the grain growth.

REFERENCES

1. M. Matsuoka, "Nonohmic Properties of ZnO Ceramics," *Jpn. J. Appl. Phys.*, **10** (6) 736-746 (1971).
2. M. Matsuoka, "Progress in Research and Development of ZnO Varistor," pp. 290-308 in

- Adv. Ceram., Vol. 1, 1981.
3. L.M. Levinson and H.R. Philipp, "ZnO Varistors for Transient Protection," IEEE Trans. Parts. Hybrid Packaging pap-13, 338 (1977).
4. J. Wong and W.G. Morris, "Microstructure and Phases in Nonohmic ZnO-Bi₂O₃ Ceramics," *Ceram. Bull.*, **53** (11), 816-820 (1974).
5. M. Inada, "Microstructure of Nonohmic Zinc Oxide Ceramics," *Jpn. J. Appl. Phys.*, **17** (4) 673-677 (1978).
6. C.N.R. Rao, G.V.S. Rao and S. Ramdas, "Phase Transformations and Electrical Properties of Bismuth Sesquioxide," *J. Phys. Chem.*, **73** (3) 672-75 (1969).
7. H. Kanai, M. Imai and T. Takahashi, "A High-Resolution Transmission Electron Microscope of a ZnO Varistor," *J. Mat. Sci.*, **20** 3957-66 (1985).
8. J. Wong, "Microstructure and Phase Transformation in Highly Nonohmic Metal Oxide Varistor Ceramics," *J. Appl. Phys.*, **46** (4) 1653-59 (1975).
9. M. Inada, "Crystal Phases of Nonohmic ZnO Ceramics," *Jpn. J. Appl. Phys.*, **17** (1) 1-10 (1978).
10. H. Kanai and M. Imai, "Effect of SiO₂ and Cr₂O₃ on the Formation Process of ZnO Varistors," *J. Mat. Sci.*, **23**, 4379-82 (1988).
11. K.N. Kim and S.M. Han, "The Effects of Intergranular Layer on the Nonohmic Characteristics of ZnO-Bi₂O₃ Ceramics," *J. Kor. Ceram. Soc.*, **26** (4) 487-492 (1989).
12. Jinho Kim, T. Kimura, and T. Yamaguchi, "Effect of Bismuth Oxide Content on the Sintering of Zinc Oxide," *J. Am. Ceram. Soc.*, **72** (8) 1541-44 (1989).
13. M.I. Mendelson, "Average Grain Size in Polycrystalline Ceramics," *J. Am. Ceram. Soc.*, **52** (8) 443-46 (1969).